Journal of Organometallic Chemistry 770 (2014) 69–78

Contents lists available at ScienceDirect

Journal of Organometallic Chemistry

journal homepage: www.elsevier.com/locate/jorganchem

Coordination diversity of the phenazine ligand in binuclear transition metal sandwich complexes: Theoretical investigation

Meriem Merzoug [a], Bachir Zouchoune [a, b, *]

[a] Laboratoire de Chimie appliquée et Technologie des Matériaux, Université Larbi Ben M'Hidi-Oum el Bouaghi, 04000 Oum el Bouaghi, Algeria
[b] Unité de Recherche de Chimie de l'Environnement et Moléculaire Structurale, Université-Constantine 1 (ex Mentouri-Constantine), Algeria

ARTICLE INFO

Article history:
Received 23 May 2014
Received in revised form
28 July 2014
Accepted 30 July 2014
Available online 19 August 2014

Keywords:
Electronic structure
Bonding analysis
Density functional theory
Coordination chemistry
Natural bond analysis
Energy decomposition analysis

ABSTRACT

DFT calculations with full geometry optimization have been carried out for all the low-energy isomers of $[M(C_{12}N_2H_8)]_2$ (M = Sc–Ni and $C_{12}N_2H_8$ = phenazine ligand = Phz). Depending on the metal atoms, phenazine adopts various hapticities that involve full or partial coordination of the C_6 and C_4N_2 rings. Phenazine is also shown to be quite flexible with respect to the spin ground state. The phenazine ligand can be bound to the metals involving its C_6 and C_4N_2 rings or its outer C_6 ones through various coordination modes such as η^4–η^4, η^6–η^4 and η^6–η^6, giving rise to the conformations of types (**a**) and (**b**). This study has shown that the electronic communication between the metal centers depends on their oxidation state in harmony with the neutral, monoanionic and dianionic phenazine forms. The major structures showed the preference of the coordination in separate way of the metal centers apart from the Ti, V and Co ones. The MO plots, WBIs (Weber bond indices) obtained from the Weinhold nature bond order analysis and the metal–metal bond lengths gave a deeper insight on the metal–metal bonding. Energy decomposition analysis showed that the interactions in the studied compounds are governed by half covalent and half electrostatic character.

Introduction

The discovery of the ferrocene in 1951 [1], has given rise to wide investigations of more metallocenes with various transition metals [2,3]. Nevertheless, the major part of these investigations has turned around the sandwich and half-sandwich mononuclear complexes containing transitional metals coordinating diverse ligands [4–24]. To the best of our knowledge, the studies about dimetallocene are less investigated. Thus, it is surprising to note the scarcity of polymetallic sandwich compounds in which several metals are sandwiched between two fused polycyclic or heteropolycyclic systems. The pioneering work of Kaltz and co-workers has highlighted the first examples of iron binuclear sandwich compound Fe_2(as-indacene)$_2$ in 1964 [25], followed hereafter by the isolation of the bis(pentalene) nickel and cobalt complexes [26]. Since, an important number of binuclear sandwich compounds of various monocyclic (cot) [27,28] or polycyclic (pentalene, indenyl and fulvalene) ligands have been isolated [29–37]. Recently, another sandwich compound has been synthesized and characterized, where two cobalt atoms are encapsulated into a rigid cage of two indenyl ligands [38]. However, Murahashi et al. have extensively investigated the polypalladium sandwich complexes in the last decade [39–42]. In this regard, we were, thus, encouraged to explore the field involving hetero-polycyclic ligands such as phenazine. On the basis of the success of previous experimental [43–48] and theoretical studies [49] of the transition metal π-bonded complexes involving carbon and nitrogen atoms, we were interested in the development of the phenazine ligand's coordination chemistry of binuclear sandwich complexes. The free phenazine molecule is an aromatic electron donating system (14 π-electrons), which is structurally related to and isoelectronic with acridine and anthracene presenting a delocalized scheme in accordance with a formal bond order of 1.5 [43]. Assuming that a binuclear complexation occurs either at the two C_6 rings or at C_6 and C_4N_2 rings, it appears from Scheme 1, that the phenazine can provide only a maximum of 10 or 12 π-electrons among 14 to the metal centers.

Phenazine is among the organic molecules that possess large and delocalized π systems capable of embarking in a significant charge transfer interaction with a transition metal, which is

* Corresponding author. Laboratoire de Chimie appliquée et Technologie des Matériaux, Université Larbi Ben M'Hidi-Oum el Bouaghi, 04000 Oum el Bouaghi, Algeria. Tel.: +213 6 62038183; fax: +213 32 423983.
E-mail addresses: b.zouchoune@univ-oeb.dz, bzouchoune@gmail.com (B. Zouchoune).

http://dx.doi.org/10.1016/j.jorganchem.2014.07.025
0022-328X/

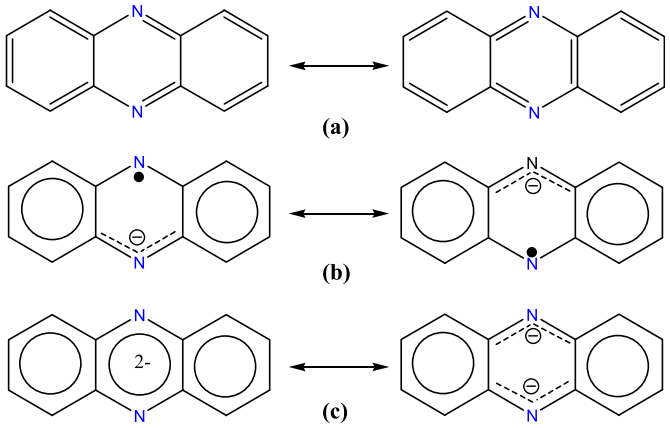

Scheme 1. Lewis representation of neutral (a), monoanionic (b) and dianionic (c) forms of the phenazine ligand.

particularly versatile, since it may act both as a regular neutral donor and a reduced ligand acting as mono- or dianion species, whose Lewis formula are shown in Scheme 1, engaging in electron transfer reactions with a wide variety of elements. Thus, it is involved in many electron transfers due to its easy reducible nature and can form complexes with transition metals [44]. In fact, the most attractive feature of these molecules as ligands is their aptitude to act as electron reservoir and to transfer spin density on require to and from the metal center. The main purpose of this work is the studying by means of DFT method the predicted low-lying states obtained by the interactions between the two phenazine rings in their various forms and the transition metals of the first row (Sc–Ni) in their different spin states. The metal–metal bonding is analyzed by using the molecular orbital plots and NBO method based on the WBIs (Wiberg bond indices).

Molecular structures

Depending simultaneously on the metal center positions and on the two phenazine ligands disposition, three structures are possible of the complexes of general formula $[M(Phz)]_2$ (M = Sc, Ti, V, Cr, Mn, Fe, Co, Ni and Phz = Phenazine), such as shown in Scheme 2. When

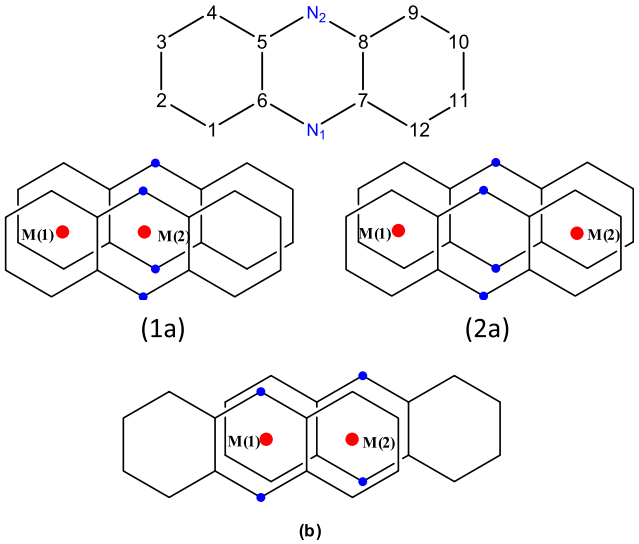

Scheme 2. Atom labeling used throughout this paper and the projected $[M(Phz)]_2$ structures of conformations (**1a**), (**2a**) and (**b**).

both phenazine ligands are totally eclipsed, one metal center can be coordinated to one C_6 ring of each phenazine, while the second metal can coordinate either C_4N_2 ring of each phenazine (conformation of type (**1a**)) or the remaining C_6 ring of each phenazine (conformation of type (**2a**)). The third possibility corresponds to the coordination to the neighboring C_6 and C_4N_2 rings in a partially eclipsed arrangement (conformation of type (**b**)). The (**1a**) and (**b**) conformations offer the possibility of direct metal–metal bonding. The geometries of the complexes $[M(Phz)]_2$ were optimized in their lowest states. The computed data are gathered in Tables 1 and 2 and selected optimized molecular structures are shown in Figs. 1, 3–9.

Results and discussion

$[Sc(Phz)]_2$ complexes

The $[Sc(Phz)]_2$ species are the less rich in electrons of the first row transition metals $[M(Phz)]_2$ series. For all conformations, the π-electrons of the coordinated rings are shared equitably by the two metals in conformity with the short Sc–C and Sc–N bond distances such as shown in Fig. 1 and in Supplementary information. Surprisingly, the singlet spin state $[Sc(\eta^6,\eta^6\text{-Phz})]_2$ (**2a**), structure with C_s symmetry where both scandium metals are coordinated to the terminal C_6 rings of each phenazine is calculated as the most stable isomer. For such coordination mode, one phenazine ligand can be described as dianionic, but the second is considered as neutral, giving rise to monovalent Sc(I) metals. This global minimum structure displays strong Sc–C interactions, where the distances range from 2.443 to 2.572 Å giving an average 2.507 Å (See Supplementary information). These bond distances are in accordance with a perfect η^6 coordination mode of each coordinated ring, matching well with the neglected slippage of 9%. A small HOMO–LUMO gap of 0.34 eV is computed for this structure. The triplet spin state of the same conformation (**b**) is obtained less stable than the global minimum by 17.2 kcal/mol. For the latter isomer each of the two unpaired electrons is located on one metal center, showing a disfavored paramagnetic behavior than the diamagnetic.

Usually, the deficient structures tend to form metal–metal bonds in order to gain more stability and compensate the metallic need in electrons. However, it is not the case for the $[Sc(\eta^6,\eta^6\text{-Phz})]_2$ (**1a**) singlet spin state structure with C_{2v} symmetry, which is expected to present triple metal–metal bond to reach a 16-MVE configuration for each Sc center. The Sc–Sc bond length of 3.225 Å, the MO plots (σ metal–metal bonding is occupied, but where π, δ, π*, δ* and σ* are vacant) and WBI of 0.18 (Wiber Bond Index), which is determined by Natural Bond Orbital (NBO) analysis [50] (with NBO 5.0 program) [51] show the presence of only a single bond following the electronic configuration: $(\sigma)^2(\pi)(\delta)^0(\sigma^*)^0(\pi^*)^0(\delta^*)^0$. The structure's distortion is accompanied by a relative instability witnessed by an important folding angles of 30° (C(6)N(1)N(2)C(8) and C(6′)N(1′)N(2′)C(8′) dihedral angles). This distorted arrangement is due to strong π-π repulsions between the uncoordinated C_6 rings of the two phenazine ligands evidenced by the long distance $d_{Rcent\ldots R'cent}$ = 5.130 Å (Rcent = center of the C_6 ring), which disfavors the face-to-face arrangement. These π–π repulsions are well shown in Fig. 2(1), where $21a_2$ and $29b_2$ orbitals highlight clearly the antibonding character between the uncoordinated C_6 rings. The Sc–Sc bond length of 3.225 Å corresponds to a single bond, in agreement with the calculated NBO of and the MOs localization showing only σ Sc–Sc bonding orbital ($38a_1$). Therefore, the weak M–M bonding is associated with small HOMO–LUMO gap of 0.73 eV. The triplet spin state structure of the same conformation (**1a**) lies 6.3 kcal/mol above the corresponding spin state and 17.7 kcal/mol higher than the global minimum, but

Table 1
Selected parameters of various $[M(Phz)]_2$ (M = Sc, Ti, V) structures with different conformations.

	Symmetry and spin state		HOMO–LUMO gap (kcal/mol)	Relative energy (eV)	M(1)–M(2) (Å)	WBI	Averaged M(1)–C (Å)	Averaged M(2)–C (Å)	Averaged M–N (Å)
$Sc_2(Phz)_2$	C_{2v} (**1a**)	$S = 0$	0.73	11.4	3.225	0.185	2.527	2.552	2.311
		$S = 1$	–	17.7	3.114	0.192	2.545	2.525	2.344
	C_s (**2a**)	$S = 0$	0.34	0.00	–		2.507		–
		$S = 1$	–	17.2	–		2.517		–
	C_{2h} (**b**)	$S = 0$	0.23	17.0	2.892	0.402	2.536	2.536	2.265
		$S = 1$	–	11.8	3.041	0.025	2.553	2.553	2.264
$Ti_2(Phz)_2$	C_{2v} (**1a**)	$S = 0$	0.40	7.8	2.765	0.630	2.376	2.372	2.218
		$S = 1$	–	12.1	2.563	0.330	2.378	2.382	2.271
	D_{2h} (**2a**)	$S = 0$	0.42	15.1	–		2.353	2.353	–
		$S = 1$	–	17.6	–		2.374	2.374	–
	C_{2h} (**b**)	$S = 0$	0.58	0.00	2.639	0.812	2.390	2.390	2.159
		$S = 1$	–	4.9	2.617	0.309	2.403	2.403	2.206
$V_2(Phz)_2$	C_{2v} (**1a**)	$S = 0$	0.80	4.6	2.511	1.310	2.230	2.317	2.193
		$S = 2$	–	12.2	2.961	0.191	2 0.301	2.390	2.197
	D_{2h} (**2a**)	$S = 0$	0.17	20.1	–	–	2.293	2.293	–
		$S = 1$	–	4.2	–	–	2.315	2.314	–
		$S = 2$	–	0.0	–	–	2.340	2.340	–
	C_{2h} (**b**)	$S = 0$	0.5	5.3	2.532	1.360	2.315	2.315	2.186
		$S = 1$	–	4.8	2.618	0.200	2.327	2.327	2.204
		$S = 2$	–	18.0	2.800	0.162	2 0.343	2.343	2.186

Table 2
Selected parameters of $[M(Phz)]_2$ (M = Cr, Mn, Fe, Co, Ni) structures with different conformations.

	Symmetry and spin state		HOMO-LUMO gap (kcal/mol)	Relative energy (eV)	M(1)–M(2) (Å)	WBI	Averaged M(1)–C (Å)	Averaged M(2)–C (Å)	Averaged M–N (Å)
$Cr_2(Phz)_2$	C_s (**1a**)	$S = 1$	–	7.9	2.748	0.012	2.219	2.368	2.168
		$S = 2$	–	14.8	2.703	0.109	2.283	2.401	2.209
	C_s (**2a**)	$S = 1$	–	0.0	–	–	2.250	2.252	–
	D_{2h} (**2a**)	$S = 2$	–	1.9	–	–	2.214	2.214	–
	C_{2h} (**b**)	$S = 2$	–	21.0	2.668	0.178	2.325	2.325	2.164
		$S = 1$	–	12.5	2.687	0.057	2.272	2.272	2.182
$Mn_2(Phz)_2$	C_{2v} (**1a**)	$S = 0$	1.05	34.0	2.773	0.230	2.203	2.242	2.164
		$S = 1$	–	38.1	2.577	0.047	2.269	2.326	2.212
	D_{2h} (**2a**)	$S = 1$	–	14.7	–		2.216	2.216	–
	C_s (**2a**)	$S = 0$	0.95	0.0	–		2.201	2.201	–
	C_{2h} (**b**)	$S = 0$	1.07	33.8	2.759	0.400	2.196	2.196	2.165
		$S = 1$	–	44.4	2.615	0.280	2.267	2.233	2.218
$Fe_2(Phz)_2$	C_s (**1a**)	$S = 0$	1.06	34.4	2.614	0.230	2.219	2.135	2.211
	C_1 (**1a**)	$S = 1$	–	26.9	2.734	0.100	2.117	2.339	2.352
		$S = 0$	0.23	30.0	2.696	0.490	2.116	2.131	1.885
	D_{2h} (**2a**)	$S = 0$	0.27	4.3	–		2.195	2.195	–
	C_s (**2a**)	$S = 1$	–	8.7	–		2.195	2.195	–
		$S = 0$	0.68	0.0	–		2.177	2.183	–
		$S = 1$	–	8.5	–		2.141	2.141	–
	C_{2h} (**b**)	$S = 0$	0.13	45.5	2.653	0.250	2.245	2.245	2.198
		$S = 1$	–	32.4	2.898	0.080	2.210	2.210	2.233
$Co_2(Phz)_2$	C_{2v} (**1a**)	$S = 0$	0.44	35.6	2.686	0.470	2.182	2.241	2.255
	C_1 (**1a**)	$S = 1$	–	22.5	2.590	0.060	2.198	2.209	2.356
		$S = 0$	0.65	0.0	2.656	0.310	2.142	2.139	1.935
		$S = 1$	–	5.3	2.922	0.003	2.171	2.148	1.941
	D_{2h} (**2a**)	$S = 0$	0.18	16.4	–	–	2.164	2.164	–
		$S = 1$	–	0.0	–	–	2.232	2.232	–
	C_{2h} (**b**)	$S = 0$	0.75	28.7	3.281	0.004	2.213	2.213	2.224
$Ni_2(Phz)_2$	D_{2h} (**2a**)	$S = 0$	0.23	0.0	–	–	2.189	2.189	–
		$S = 1$	–	4.8	–	–	2.256	2.256	–
	C_{2h} (**b**)	$S = 0$	0.47	16.9	4.402	–	2.183	2.183	–
		$S = 1$	–	28.8	2.731		2.143	2.143	–

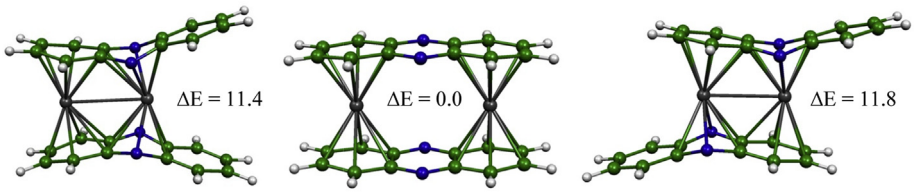

Fig. 1. Optimized $[Sc(Phz)]_2$ structures of the most stable isomer for each conformation. Relative energies between isomers are given in (kcal/mol).

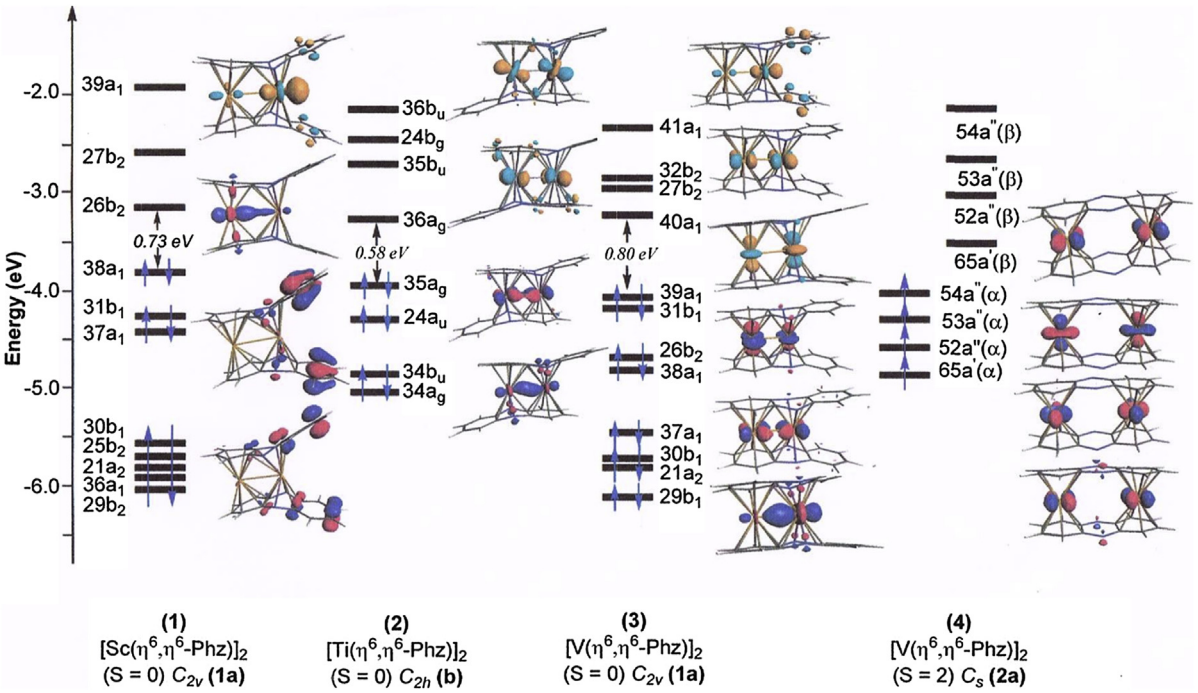

Fig. 2. MO diagrams obtained for $[Sc(\eta^6,\eta^6\text{-Phz})]_2$ ($S = 0$) C_{2v}, $[Ti(\eta^6,\eta^6\text{-Phz})]_2$ ($S = 0$) C_{2h}, $[V(\eta^6,\eta^6\text{-Phz})]_2$ ($S = 0$) C_{2v} and $[V(\eta^6,\eta^6\text{-Phz})]_2$ ($S = 2$) C_s. Contour values of MO plots are ±0.06 (e/bohr^3).

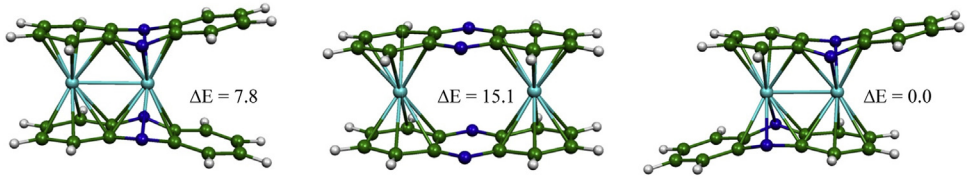

Fig. 3. Optimized $[Ti(Phz)]_2$ structures of the most stable isomer for each conformation. Relative energies between isomers are given in (kcal/mol).

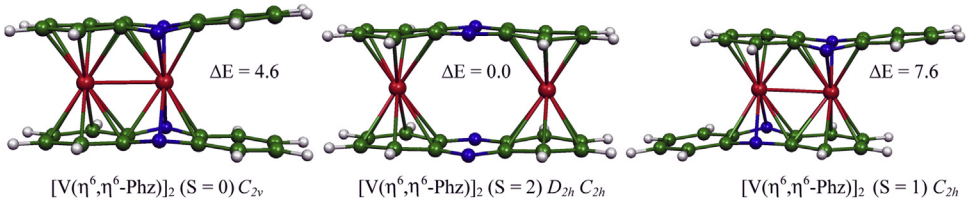

Fig. 4. Optimized $[V(Phz)]_2$ structures of the most stable isomer for each conformation. Relative energies between isomers are given in (kcal/mol).

presenting a relative short Sc–Sc bond distance of 3.114 Å against 3.225 Å for the single state. It is worth noting that the decreasing of Sc–Sc bond length of the triplet spin state structure agrees well with the depopulation of the HOMO which exhibits an antibonding M–M character showing a slight enhancement of the WBI of 0.192 against 0.185 of the singlet spin state structure.

Likewise, $[Sc(\eta^6,\eta^6\text{-Phz})]_2$ (**b**) singlet and triplet states structures of C_{2h} symmetry are optimized as energy minimum, but less stable than the global minimum by 17.0 and 11.8 kcal/mol, respectively, displaying a relatively long Sc–C and Sc–N bond lengths compared to those calculated of (**1a**) and (**2a**) structures (See Supplementary information). For each optimized structure, we note that the lowering of C_{2v}, C_{2h} and D_{2h} symmetries to C_1 one does not provoke structural distortion and the calculated total bonding energies are comparable.

$[Ti(Phz)]_2$ complexes

The $[Ti(Phz)]_2$ complexes series possesses two supplementary electrons than the $[Sc(Phz)]_2$ ones, thus occupying an additional MO, which in principle induces metal–metal bonding, but remain as electron deficient species. For each conformation, two isomers (one singlet and one triplet) are optimized as energy minimum structures such as shown in Fig. 3, Table 1 and Supplementary information. Indeed, the singlet spin state $[Ti(\eta^6,\eta^6\text{-Phz})]_2$ (**b**) structure with C_{2h} symmetry is calculated as the most stable isomer

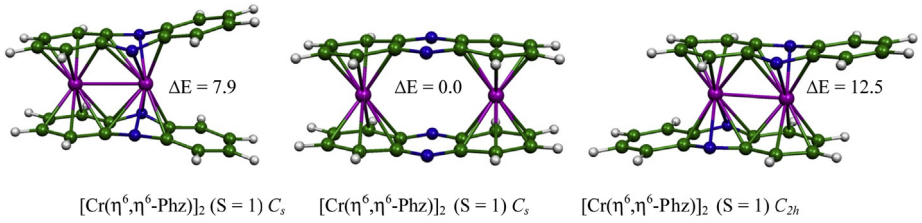

Fig. 5. Optimized $[Cr(Phz)]_2$ structures of the most stable isomer for each conformation. Relative energies between isomers are given in (kcal/mol).

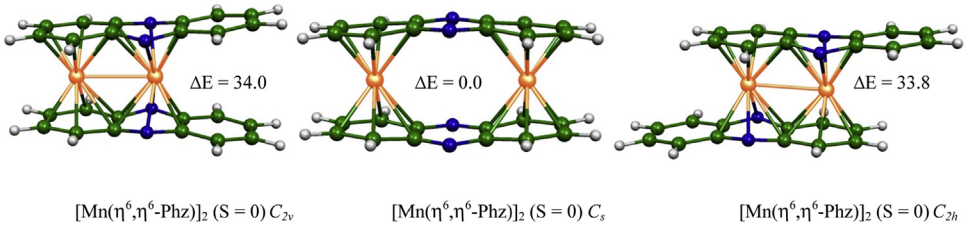

Fig. 6. Optimized geometries of $[Mn(Phz)]_2$ in their singlet and triplet states. Relative energies between isomers are given in (kcal/mol).

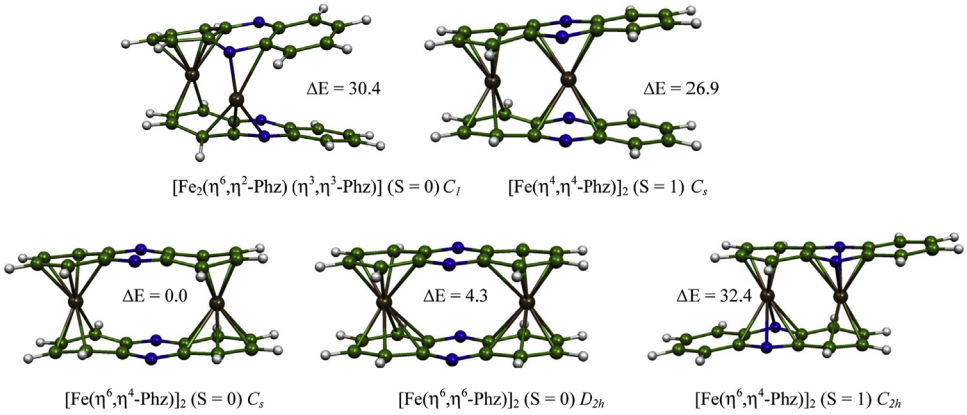

Fig. 7. Optimized $[Fe(Phz)]_2$ structures of the most stable isomer for each conformation. Relative energies between isomers are given in (kcal/mol).

corresponding to the partially eclipsed arrangement. For this global minimum structure, both Ti metal centers are equivalent by symmetry. In fact, they are described by a perfect η^6,η^6 coordination mode, showing the involvement of the two adjacent C_6 and the C_4N_2 rings of both phenazine ligands, hence, involving twenty π-electrons in the interaction with the metals. The obtained η^6,η^6 coordination mode is witnessed by strong interactions between neutral phenazine ligands and titanium metals, where short Ti–C bond distances are in the range of 2.387–2.416 Å (See Supplementary information) giving an average bond distance of 2.400 Å and Ti–N ones are of 2.159 Å. For this global minimum, the short Ti–N bond length indicates strong interaction through nitrogen atoms, thus, emphasizing the involvement of this type of atom as has been demonstrated in previous theoretical investigations [21–23] and [46,47]. This global minimum structure is marked by an important distortion evidenced by a folding angle of 28°, giving, thus, a non-planar arrangement of the phenazine

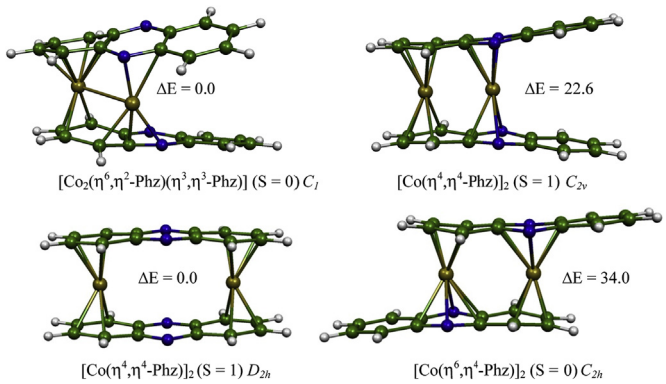

Fig. 8. Optimized $[Co(Phz)]_2$ structures of the most stable isomer for each conformation. Relative energies between isomers are given in (kcal/mol).

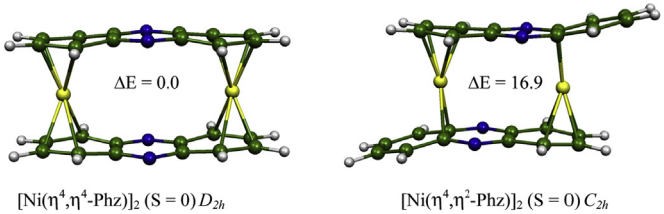

Fig. 9. Optimized $[Ni(Phz)]_2$ structures of the most stable isomer for each conformation. Relative energies between isomers are given in (kcal/mol).

ligands. The energetic parameters gathered in Table 1 show a relatively small HOMO–LUMO gap of 0.58 eV for the optimized singlet spin state [Ti(η^6,η^6-Phz)]$_2$ structure, which is slightly more stable than its corresponding triplet state by 4.9 kcal/mol. Molecular orbital analysis provides a useful tool to establish M–M bond order, in this regard, the electronic configuration stemming from the MOs diagram (Fig. 2(2)) corresponds to $(\sigma)^2(\pi)^2(\delta)^0(\sigma^*)^0(\pi^*)^0(\delta^*)^0$. This electronic configuration corroborates the presence of Ti–Ti double bond of 2.639 Å, in accordance with a formal bond order of 2 consisting of one σ ($34a_g$) bond and one π ($24a_u$) bond, which leads to 16-/16-MVE of each metal center. This bond order is confirmed by NBO calculations which gave a WBI value of 0.812, consistent with the hypothesis developed previously. The σ Ti–Ti bond is made by a combination of d_z^2 and $d_{x^2-y^2}$ AOs, while the π Ti–Ti one is formed by pure metallic d_{yz} AOs of each metal as depicted in Fig. 2. Finally, the singlet spin state is calculated as the ground state for the [Ti(η^6,η^6-Phz)]$_2$ structures independently of the conformation. This electronic deficiency is equitably delocalized on the two metallic atoms considered as 16-/16-MVE centers responding to the electronic configuration given previously. The triplet spin state of the conformation (**b**) corresponds to the following electronic configuration $(\sigma)^2(\pi)^1(\pi^*)^1(\delta)^0(\sigma^*)^0$ $(\delta^*)^0$ is less stable by 4.9 kcal/mol than the global minimum. One can observe the similarities for the Ti–C and Ti–N bond lengths between the singlet and triplet spin state structures, while the Ti–Ti bond distance undergoes a slight shortness (2.617 *vs* 2.639 Å). As can be seen from Table 1, there is no linear relationship between the bond orders and the bond lengths. Indeed, the shortest Ti–Ti bond distance of 2.039 Å corresponds to the smallest WBI of 0.309.

The different structures optimized in their totally eclipsed arrangement with conformations (**1a**) and (**2a**) are less stable than the global minimum of C_{2h} symmetry. Indeed, the singlet and triplet states of the conformation (**1a**) lie 7.8 and 12.1 kcal/mol above the global minimum, whereas those of the conformation (**2a**) are found relatively higher in energy (Table 1). The relative instability of the conformation (**1a**) can likely be explained by the repulsions terms occurred between the two uncoordinated C_6 rings of each phenazine, where $d_{Rcent\cdots R'cent}$ = 4.451 Å (Rcent = center of the C_6 ring).

The Ti–C bond distances are in a range of 2.159–2.416 Å comparable to those structurally characterized and hypothetical binuclear complexes, while the Ti–Ti bond length of 2.639 Å corresponds to a short distance, thus, describing such bond as metal–metal double one.

[V(Phz)]$_2$ complexes

Eight optimized geometries are obtained as energy minimum for the [V(Phz)]$_2$ structures. The most stable structures for each conformation are presented in Fig. 4 (all the optimized structures are gathered in Figures of the Supplementary information) and selected parameters are given Table 1. Inversely to the eclipsed [Ti(Phz)]$_2$ structure which is the more stable in its singlet state, the totally eclipsed [V(Phz)]$_2$ (**2a**) structure with D_{2h} symmetry of quintet spin state is calculated as the most stable isomer. Indeed, the V(η^6, η^6-Phz)]$_2$ (**2a**) (S = 2) structure, is calculated as a global minimum, in which both outer C_6 rings are bonded to the V metals in hexacoordination η^6 manner through short V–C bond distances ranging from 2.283 to 2.456 Å, thus, marking a weak slippage of 9% towards the external carbon atoms. As can be seen from Table 1, there is no linear relationship between bond orders and bond lengths, consistent with this, there are high-lying singlet and low-lying triplet states [V(η^6, η^6-Phz)]$_2$ of the same conformation (**2a**), which lie 20.1 and 4.2 kcal/mol, respectively, above the global minimum. The singlet spin state structure displays a small HOMO–LUMO gap of 0.17 eV consistent with its relative instability compared to those of high spin. Effectively, for the quintet spin state [V(η^6, η^6-Phz)]$_2$ (**2a**) structure, the four unpaired electrons are localized on both V(+I) metals (Fig. 2(4)) which are represented by 52a″(α), 53a″(α), 64a′(α) and 54a″(α) spin orbitals, thus, nicely matching with the nature charge of +0.69. Thereby, the 16-MVE configuration is reached for both V(I) metal cations. Consequently, changing the spin state does not lead to noticeable structural modifications as can be clarified by the selected parameters in Table 1.

Surprisingly, the different isomers presenting direct V–V bonding showing a strong involvement of the nitrogen atoms are calculated slightly less stable than the structures with separated vanadium centers. Usually, the electron deficient structures are expected to form M–M bonding, in order to give rise more stable arrangements. Unfortunately, This is not the case of the vanadium structures, where the optimized structures, despite their 18-electron configuration fulfillment were calculated less stable due to the repulsion between the uncoordinated C_6 rings of phenazine ligands. The uncoordinated C_6 rings are separated by $d_{Rcent\cdots R'cent}$ = 3.969 Å, indicating that π–π repulsions are weaker than those observed for Sc and Ti structures, which somewhat explains the relative stability of this vanadium conformation compared to that obtained for scandium and titanium, thus the energy difference is reduced between C_{2v} and D_{2h} symmetries.

As can be seen from the selected parameters of the structure gathered in Table 1, the singlet spin state structure lies 4.6 kcal/mol above the global minimum displaying a significant HOMO–LUMO of 0.80 eV and relatively short V–C bond distances ranging from 2.267 to 2.336 Å compared to those obtained of the D_{2h} symmetry isomers. The findings attribute a 18-/18-MVE configuration of vanadium metals, which is reached by assuming a V–V triple bond of 2.541 Å, consistent with MOs localization as sketched in Fig. 2(3). This bond distance is somewhat short and consistent with the calculated bond order of 1.33 suggesting a triple V–V bonding and comparable to that found in previous work for the [V(Az)]$_2$ [13]. These results match very well with the electronic configuration: $(\sigma)^2(\pi)^2(\delta)^2(\sigma^*)^0(\pi^*)^0(\delta^*)^0$ showing the occupation of the σ($37a_1$), π($26b_2$) and δ($39a_1$) bonding orbitals and the depopulation of their antibonding counterparts σ*($41a_1$), π*($27b_2$) and δ*($40a_1$) of d_z^2, d_{yz} and $d_{x^2-y^2}$ characters, respectively (see Fig. 2(3)), following the Wiberg bond index of 1.36. It is important to note that the triplet spin state isomer of C_{2v} symmetry is not identified as energy minimum, where a large imaginary frequency is calculated. Changing the spin state does not substantially affect the geometrical structures. Really, for the quintet spin state the bond distance deviation does not exceed 7%, however, the WBI falls from 1.310 to 0.191 for the triplet spin state in agreement with the $(\sigma)^2(\pi)^1(\delta)^1(\delta^*)^1(\pi^*)^1(\sigma^*)^0$ electronic configuration. One can observe for this electronic configuration the depopulation of the π and δ MOs, which agrees well with a double V–V single bond length which increases from 2.541 (singlet spin state) to 2.961 Å (quintet spin state).

[Cr(Phz)]$_2$ complexes

The [Al(Et)$_2$Cr(Phz)]$_2$ is the alone experimentally characterized complexed as a sandwich bimetallic species of the phenazine ligand, where both chromium atoms are encapsulated into a rigid cage of two phenazine ligands and the two Al(Et)$_2$ substituents each bridge a pair of nitrogen atoms [52]. The optimized [Cr(Phz)]$_2$ considered as an unsubstituted structures are displayed in Fig. 5 (only the most stable structure of each conformation is given, but all the optimized structures for different spin states and different

conformations are given in the Supplementary information) and the energetic parameters gathered in Table 2, show that the isomers of high spin state ($S = 1$ and $S = 2$) are found as energy minimum regardless the conformation and the symmetry. However, the singlet spin state structures do not correspond to ground states whatever the conformation. The triplet spin state [Cr(η^6, η^6-Phz)]$_2$ (**2a**) structure with C_s symmetry which is derived from D_{2h} is calculated as the most stable isomer with the metal centers coordinating the outer C_6 rings in η^6 manner. In such structure, the imposed C_s symmetry generates an unsymmetrical phenazine ligands, with one is described as dianionic and the second as neutral species, thus conducting to low spin Cr(+I) monocation centers as encountered in chromium arene complexes [53,54]. The perfect η^6 coordination mode is consistent with the short Cr–C bond lengths ranging from 2.189 to 2.340 Å giving an average bond of 2.250 Å (See Supplementary information), in accord with the weak slippage which does not exceed 8%. In such situation, each phenazine donates twelve π electrons to the Cr pair atoms giving to both metal centers the 17-MVE configuration. The quintet spin state isomer with the same conformation lies only 1.9 kcal/mol above the global minimum. The comparable total bonding energies and geometrical parameters between these two isomers arises chiefly from the localization of the unpaired electrons in both triplet and quintet spin sates, which occupy nonbonding metal orbitals. Varying the spin state, would not modify the geometrical parameters. However, the C_{2v} and C_{2h} structures coordinating the adjacent C_6 and C_4N_2 rings, offering the possibility of direct metal–metal bonding are disfavored compared to those of the separated metal centers. The corresponding C_{2v} and C_{2h} triplet state arrangements are slightly distorted evidenced by the calculated folding angles of 14 and 17°, respectively. For each predicted structure with C_{2v} and C_{2h} symmetries, the Cr–Cr bond lengths of 2.748 and 2.687 Å, do not suggest metal–metal bonding. The Cr(1) metal exhibits an η^6,η^6 coordination mode is considered as monocation Cr(+I) reaching a 17-MVE configuration in accordance with the calculated natural charge of +0.65. The second Cr(2) is described by an η^4,η^4 coordination mode behaves as monoanion Cr(−I) acquiring a natural charge of −0.80. Inversely to the quintet spin state structure of D_{2h} symmetry which is in flat potential energy surface with the global minimum, those of C_{2v} and C_{2h} symmetries are 14.8 and 21.0 kcal/mol higher in energy than the global minimum. Finally, we note that the difference in energies between the high symmetry structures and those of C_1 one does not exceeds 2 kcal/mol.

[Mn(Phz)]$_2$ complexes

The geometry optimizations carried out on the [Mn(Phz)]$_2$ whatever the conformation and the symmetry have revealed that the singlet spin state structures are more stable than those of the triplet and quintet spin state ones, as displayed in Fig. 6 (only the most stable structure of each conformation is given in Fig. 6, more details are given in the Supplementary information) and Table 2. The molecular [Mn(η^6, η^6-Phz)]$_2$ (**2a**) structure with C_s symmetry derived from that of D_{2h} demonstrates that both Mn centers coordinating the outer C_6 rings in an η^6 manner corresponds to the most stable isomer with unsymmetrical phenazine ligands. This coordination mode would give to each Mn center an 18-MVE configuration as monovalent cation. This situation generates one phenazine as dianionic and the second one as neutral species. This global minimum energy structure exhibits a significant HOMO–LUMO gap of 0.97 eV consistent with short Mn–C bond lengths ranging from 2.111 to 2.334 Å (see Supplementary information), leading to a weak slippage of each metal center of $\delta = 9\%$. Its corresponding triplet state lies 14.7 kcal/mol higher in energy giving rise to a species with 17-/17-MVE metal center as divalent Mn(II) cations and exhibits relatively long M–C bond distances, but small metal centers slippage ($\delta = 7\%$). The different isomers corresponding to the coordination of the neighboring C_6 and C_4N_2 rings with C_{2v} and C_{2h} symmetries in their singlet spin state are obtained very high in energy lying 34.0 and 33.8 kcal/mol above the global minimum, this despite the presence of a weak Mn–Mn bond with WBI of 0.23 and 0.40, respectively. However, their homologues of triplet spin state are much higher in energy than the global minimum (Table 2). These findings show the preference of the coordination of the separated rings than those of the adjacent ones. It worth noting that for each optimized structure, the lowering of C_{2v}, C_{2h} and D_{2h} symmetries to C_1 one does not provoke structural distortion, where the C_1 structures are found above those of high symmetries only about 2 kcal/mol.

[Fe(Phz)]$_2$ complexes

Firstly, the optimized geometries for [Fe(Phz)]$_2$ structures are obtained by imposing high symmetries. At this stage, the results show that the [Fe(η^6,η^6-Phz)]$_2$ isomer (D_{2h}) of the totally eclipsed conformation (**2a**) with singlet spin state is optimized as the global minimum of the energy as sketched in Fig. 7 (for details, see the Supplementary information) and Table 2. Indeed, the singlet spin state [Fe(η^6,η^6-Phz)]$_2$ (**2a**) structure lies only 4.4 kcal/mol below its triplet state isomer, in accordance with the very small HOMO/LUMO gap of 0.27 eV conferring a closed shell configuration. For this structure each Fe atom is bonded to one terminal C_6 ring of each phenazine ligand in η^6 manner. Such situation agrees with the Fe–C bond distances ranging between 2.083 and 2.361 Å (see Supplementary information). This coordination mode of iron metals, let us to consider each phenazine molecule as a dianion ligand in accordance with the Lewis Scheme 1(b), giving rise to a configuration of 18-/18-MVE to both metals in (+2) valent state leading to a diamagnetic behavior. Thus, it is also likely to consider the complex as constructed by two phenazines; each in dianionic form, coordinated to two transition metals. The [Fe(η^6,η^6-Phz)]$_2$ triplet state structure with low C_s symmetry lies only 4.4 kcal/mol above its homolog of singlet spin state with nonequivalent phenazine ligands, allowing the metals to reach the 17-/17-MVE configuration with monovalent oxidation state. This situation corresponds to one neutral phenazine and another dianionic species. For this triplet state, each of the two unpaired electrons is localized on each iron metal. Interestingly to mention that the lowering of the D_{2h} symmetry to the C_s one, generates the most stable [Fe(η^6,η^4-Phz)]$_2$ (**2a**) isomer with an η^6,η^4 coordination mode rather than η^6,η^6, leading to a partial decoordination of one C_6 ring of each phenazine ligand. In this case, both iron metals are in 18-MVE closed shell configuration, while the phenazine are described as neutral ligands presenting a distorted structure evidenced by the folding angle between the C_6 and C_4N_2 rings ($\theta = 19°$). The [Fe(η^6,η^4-Phz)]$_2$ global minimum isomer C_s is more stable than that of the high D_{2h} symmetry by 4.3 kcal/mol, but exhibiting a relatively large HOMO–LUMO gap of 0.68 eV. The regular coordination mode is in agreement with the short Fe–C bond distances ranging from 2.055 to 2.236 Å. For this structure, the lowering of the D_{2h} symmetry to the C_s one is marked by considerable lengthening of four Fe–C bond lengths from 2.361 to 2.656 Å leading to the rupture of Fe(1)–C(5′), Fe(1)–C(6′), Fe(2)–C(5) and Fe(2)–C(6) bonds.

In contrast, the coordination of the neighboring C_6 and C_4N_2 rings with a perfect η^4,η^4 coordination mode gives rise to disfavorable structures, which are expected to provide more stable isomers by direct metal–metal bond formation. As can be seen from Fig. 7 and Table 1, it is clear that these structures are less stable than those of separated iron centers arrangements, where the

isomers of (C_{2v}) and (C_{2h}) lie 34.4, 26.9, 45.5 and 32.4 kcal/mol above the global minimum [Fe(η^6,η^4-Phz)]$_2$ singlet state isomer of C_s symmetry, respectively. To this regard, M–C bonding is preferred over M–M and M–N bonding leading to more stable structures of separated coordinated rings than those of adjacent ones. Furthermore, this relative instability is due to the π–π repulsions between the uncoordinated C_6 rings, which search the remote positions from each other.

The singlet spin state optimized structure of type (**1a**) without constraint of symmetry (Fig. 7) is found slightly more stable by 4.0 kcal/mol than that of the same type with (C_s) symmetry, but less stable by 30.4 kcal/mol than the global minimum in accordance with the small HOMO–LUMO gap of 0.23 eV. This unsymmetrical structure is described by a distorted arrangement with an originate (η^6,η^2) and (η^3,η^3) coordination modes of the phenazine ligands giving rise to monovalent Fe(I) metals in concordance of the nature charges of +0.44 and +0.62. This situation is described by one Fe(1) and Fe(2) metals acquiring 18 and 16-MVE, respectively, bound by a weak Fe–Fe single bond of 2.696 Å which matches well with the calculated WBI of 0.490.

[Co(Phz)]$_2$ complexes

The most stable isomer of [Co(Phz)]$_2$ species corresponds to the totally eclipsed configuration (**2a**) indicating an η^4 coordination mode of the two terminal C_6 rings of both phenazine ligands. This type of coordination leads to important slippage of 12% towards the external C(3), C(4), C(10), C(11), C(3′), C(4′), C(10′) and C(11′) (Fig. 8). Each of the two unpaired electrons for the triplet state is localized on each cobalt metal, allowing it to reach the 17-/17-MVE configuration for both metals with zerovalent oxidation state. This situation corresponds to a neutral phenazine species with flatness geometry and short Co–C bond distances which are in the range of 2.166–2.299 Å.

The corresponding singlet spin state lies 16.4 kcal/mol above the global minimum (Table 2). This isomer displays a small HOMO–LUMO gap of 0.18 consistent with its relative instability, where short Co–C bond lengths are calculated ranging from 2.062 to 2.267 Å, showing a more pronounced slippage of 16% towards the external carbon atoms compared to those obtained for the triplet state as indicated above.

Assuming diamagnetism, a single metal–metal bond can be expected if the 18-electron rule is satisfied for both cobalt metals. The calculated intermetallic distance of 2.686 Å agrees with this hypothesis, where a weak single Co–Co bond can be attributed for this structure matching with the WBI of 0.470. However, this isomer lies 35.5 kcal/mol higher in energy than the global minimum. This relative instability can be explained by the strong π–π repulsion between the two phenazine ligands ($d_{Rcent\cdots R'cent}$ = 4.216 Å) tending to avoid the face-to-face arrangement of the uncoordinated rings. The corresponding triplet state structure is more stable lying 22.5 kcal/mol above the global minimum, but exhibiting η^4,η^6 coordination mode rather than η^4,η^4 consistent with one zerovalent Co(0) and another divalent Co(+II) in accordance with the calculated natural charges of +0.03 and +1.57, respectively, giving rise to the 17-/17-MVE open shell electronic configuration. Finally, it is worthwhile noting that the optimization without constraint of symmetry of the (**1a**) structure (Fig. 8) gave the most stable isomer, which lies at the same energy than the global minimum and displays a moderate but significant HOMO–LUMO gap of 0.65 eV. Really, the [Co(Phz)]$_2$ (S = 0) (C_1) with a distorted structure exhibits an unexpected (η^6,η^2) and (η^3,η^3) coordination mode giving rise to monovalent Co(I) metals in concordance of the nature charges of +0.78 and +0.69. This situation is described by Co(1) and Co(2) metals acquiring 18 and 16-MVE, respectively, connected by a dative Co–Co bond of 2.656 Å having a WBI of 0.310. This bonding is well described by a single σ bond (Fig. 2). Its corresponding triplet spin state displays also a distorted structure, but marked by an elongation of the Co–Co distance which becomes equal to 2.922 Å. The rupture of the metal–metal bond yield zerovalent cobalt metals with 17- and 15-MVE, where the two unpaired electrons are localized on both metals leading to the energy loss of 5.3 kcal/mol.

Table 3
Results of the energy decomposition analysis for the [M(Phz)]$_2$ (M = Sc, Ti, V, Mn, Fe, Co and Ni) obtained at BP86/TZP.[a]

Compound	Symmetry	ΔE_{int}	ΔE_{Pauli}	ΔE_{elstat}	ΔE_{orb}
[Sc(Phz)]$_2$	C_{2v}	−570.9	643.8	−642.5 (52.9)[b]	−572.3 (47.1)[b]
	D_{2h}	−576.5	558.1	−662.6 (55.9)	−511.9 (45.1)
	C_{2h}	−545.4	623.1	−606.8 (50.9)	−560.1 (49.1)
[Ti(Phz)]$_2$	C_{2v}	614.1	733.8	−697.1 (52.0)	−650.7 (48.0)
	D_{2h}	657.2	707.7	−681.6 (50.0)	−683.3 (50.0)
	C_{2h}	−620.1	732.2	−620.1 (51.5)	−655.4 (48.5)
[V(Phz)]$_2$	C_{2v}	−638.8	777.1	−694.1 (49.0)	−721.8 (51.0)
	D_{2h}	−718.5	707.0	−696.6 (49.0)	725.9 (51.0)
	C_{2h}	−635.5	763.1	−684.6 (49.0)	714.2 (51.0)
[Mn(Phz)]$_2$	C_{2v}	−698.3	799.5	714.4 (48.0)	−783.3 (52.0)
	D_{2h}	−585.7	1701.8	−968.5 (42.4)	−1328.2 (57.6)
	C_{2h}	−695.0	798.6	−713.0 (48.0)	781.0 (52.0)
[Fe(Phz)]$_2$	C_{2v}	−291.5	1390.5	−751.3 (45.7)	−930.9 (55.3)
	D_{2h}	−387.6	1528.6	−933.5 (50.6)	−986.9 (51.4)
	C_{2h}	−331.1	1472.8	−810.6 (45.0)	−993.6 (55.0)
[Co(Phz)]$_2$	C_{2v}	−221.8	1028.5	−643.4 (51.5)	−606.7 (48.5)
	D_{2h}	−295.6	1147.5	−737.7 (55.9)	−705.4 (48.9)
	C_{2h}	−241.7	1182.3	−711.9 (50.0)	−712.1 (50.0)
[Ni(Phz)]$_2$	D_{2h}	−263.4	903.5	−610.2 (42.2)	−556.7 (47.8)

[a] Energies are given in kcal/mol.
[b] In parentheses, total attractive interactions $\Delta E_{elstat} + \Delta E_{orb}$.

[Ni(Phz)]$_2$ complexes

The optimized [Ni(Phz)]$_2$ structures with singlet spin state presented in Fig. 9 show clearly that the bonding of each Ni metal to each phenazine ligand is described by an η^4 coordination mode, thus each Ni would be satisfy the 18-electron rule. The singlet spin state isomer of D_{2h} symmetry displaying a HOMO–LUMO gap of 0.47 eV is calculated as a global minimum and lying only 3.5 kcal/mol below its homolog of triplet state. The η^4,η^4 coordination mode shows four short and four long Ni–C bond distances of 2.062 and 2.306 Å, respectively, between each metal center and both phenazine ligands. The passage from the singlet spin state to the triplet one shows an important structural modifications consisting in slipping from η^4,η^4 to η^2,η^2 for each Ni atom. This new η^2,η^2 coordination mode is obtained by the rupture of Ni–C bonds, giving rise to electronic deficient structure. Effectively, the long Ni–C bond distances of 2.306 Å obtained for the singlet spin state structure lengthen to 2.440 for the triplet spin state one. Our DFT calculations show that isomers of the eclipsed and staggered conformations coordinating the neighboring C_6 and C_4N_2 rings do not correspond to the energy minimums witnessed by the presence of large imaginary frequencies. However, those of partially eclipsed of C_{2h} symmetry with singlet spin state lie high in energy exhibiting an η^4,η^2 coordination mode as shown in Fig. 9 and Table 2.

Energy decomposition analysis

ADF program defines the molecular interaction as the energy between the molecular fragments at infinite separation and in their final positions, which are usually computed as spin restricted. Table 3, shows the results of the partitioning of the interaction ΔE_{int} energies between M_2 and $(Phz)_2$ fragments into three terms;

ΔE_{Pauli}, ΔE_{elstat}, and ΔE_{orb}. The first term ΔE_{Pauli} refers to the repulsive interactions between the fragments, which are caused by the fact that two electrons with same spin cannot occupy the same region in space. The second term ΔE_{elstat} provides the electrostatic interaction energy between the fragments, which are calculated using the frozen electron density distribution of the fragments. The last term ΔE_{orb} orbital interaction energy is the stabilizing orbital interaction tem: it is calculated in the final step of the bond decomposition energy (BDE) method [55,56] when the Kohn–-Sham orbitals relax to their optimal form, it accounts for electron pair bonding, charge transfer as exemplified by HOMO–LUMO interactions and polarization (empty/occupied orbital mixing on one fragment due to the presence of another fragment). An extensive discussion of the physical meaning of the different terms in the energy decomposition is given previous work [57]. For the same metal, one can observe from Table 3, that obtained interaction ΔE_{int} energies between M_2 and $(Phz)_2$ fragments are almost comparable, while the major tendency consists of the energy increasing progressively from Sc to Mn, hereafter it considerably decreases from Fe to Ni. The interaction ΔE_{int} energies between M_2 and $(Phz)_2$ fragments are principally related to the coordination mode of each structure. Thereby, the minimum energies are obtained for Sc, Ti, V and Mn metals displaying η^6,η^6 coordination mode, while the maximum energies correspond to the partial η^4,η^4 coordination mode for Ni. The different energy variations depend mainly on the number of M–C and M–N contacts. Indeed, for the complexes exhibiting an η^6,η^6 coordination mode, 24 × M–C (D_{2h}) or 20 × M–C and 4 × M–N (C_{2v} and C_{2h}) contacts describe the interactions between the fragments, while for the η^4,η^4 coordination mode, these contacts fall to 16 × M–C (D_{2h}) or 12 × M–C and 4 × M–N (C_{2v} and C_{2h}). It has been suggested that the relative values of the two attractive terms ΔE_{elstat}, and ΔE_{orb} may be used to characterize the nature of the chemical bonding [58]. Table 3 show comparable values between ΔE_{elstat}, and ΔE_{orb}, where ΔE_{elstat} term contributes between 48% and 52.9% except for Sc(D_{2h}) structure showing an electrostatic contribution higher by 150.7 kcal/mol, than that of orbital interaction, thus, corresponding to a slight ionic character. Inversely, ΔE_{orb} term contributes mainly in few cases (Fe(C_{2h}) 55.0%, Fe(C_{2v}) 55.3% and Mn(D_{2h}) 54.0%) corresponding to a weak electrostatic character. It is worth noting that structures of maximum interactions energies (Fe, Co and Ni) correspond to the maximum repulsive energies as shown in Table 3. It is clear that the weakening of the metal–ligand correlates well to the increase of Pauli repulsion. The obtained results gathered in Table 3 show that the difference between ΔE_{orb} and ΔE_{elstat} does not exceed 10% of the total attractive interactions $\Delta E_{orb} + \Delta E_{elstat}$. Overall, the treated compounds are governed by half covalent and half electrostatic interactions evidenced by approximately equal electrostatic and covalent character.

Computational methods

Density functional theory (DFT) calculations were carried out on the studied compounds using the Amsterdam Density Functional (ADF) program [59], developed by Baerends and coworkers [60–64]. Electron correlation was treated within the local density approximation (LDA) in the Vosko–Wilk–Nusair parametrization [65]. The non-local corrections of Becke and Perdew (BP86) were added to the exchange and correlation energies, respectively [66–69].

The numerical integration procedure applied for the calculations was developed by te Velde et al. [64]. The atom electronic configurations were described by a triple-ζ Slater-type orbital (STO) basis set for H 1s, C 2s and 2p, N 2s and 2p augmented with a 3d single-ζ polarization for C and N atoms and with a 2p single-ζ polarization for H atoms. A triple-ζ STO basis set was used for the first row transition metals 3d and 4s augmented with a single-ζ 4p polarization function. A frozen-core approximation was used to treat the core shells up to 1s for C, N and 3p for the first row transition metals [60–64]. Full geometry optimizations were carried out using the analytical gradient method implemented by Versluis and Ziegler [70]. Spin-unrestricted calculations were performed for all the open-shell systems. Frequencies calculations [71,72] were performed on all the studied compounds to check that the optimized structures are at local minima. The integration accuracy parameter was set to six. The Coulomb potential was evaluated via an accurate fitting of the charge density with Slate-type exponential functions centered on the atoms. Representation of the molecular structures and molecular orbitals were done using ADF-GUI [59] and MOLEKEL4.1 [73], respectively.

Conclusion

In this work, we have investigated the electronic and the molecular structure of [M $(Phz)_2$] sandwich complexes for the first row transition metal of the hetero-polycyclic phenazine ligand.

The coordination of the neighboring rings offers the possibility of a direct metal–metal interaction, but does not provide stabilization as expected due the strong π–π repulsions between the outer uncoordinated rings. We have shown in most cases that the direct electronic communication between the metal centers is not favored only for the Ti, V and Co. The Cr, Mn, Fe, Co and Ni metals centers prefer the coordination of the separate rings than the adjacent ones depends on their oxidation state and the attached ligands. For the deficient structures, the coordination destroys the planarity of the phenazine ligand leading to significant bent arrangements.

This study has shown that most of the investigated compounds should be “stable” enough to be isolated, so as to predict their synthesis and stimulate further theoretical and experimental investigations of π-bonded sandwich bimetallic complexes. These results show the ability of the phenazine ligand to adapt itself to the electronic demand of the metals following the nature of the metal; therefore it behaves as neutral, radical monoanionic and dianionic ligand with distorted or planar structure according to the spin state and the metal valence. It has been observed that phenazine ligand as an aromatic linker is suitable to promote metal–metal interaction if its planarity in not broken. However the loss of aromaticity decreases the electronic communication between metal centers. The predicted structures presenting direct metal–metal bond(s) were classified according to the WBI values. For the optimized structures, it turns out that M–C bonding is preferred over the M–N and M–M bonding, except for the Ti, V and cobalt structures, where the metal binding to nitrogen atoms is a stabilizing factor predicting the possible synthetic routes of π-bonded transition metal compounds. The energy decomposition analysis indicates that the electrostatic contributions are between 45 and 55% of the total attractive interactions suggesting a nearly half covalent and half electrostatic character of the studied compounds.

Acknowledgment

The authors are grateful to the Algerian MESRS (Ministère de l'Enseignement Supérieur et de la Recherche Scientifique) for the financial support. BZ thanks particularly Dr. Foued Djamai (Department of English, University of Algiers 1) for his English editing.

Appendix A. Supplementary data

Supplementary data related to this article can be found at http://dx.doi.org/10.1016/j.jorganchem.2014.07.025.

References

[1] T.J. Kealy, P.L. Pauson, Nature 168 (1951) 1039.
[2] G. Wilkinson, M. Rosenblum, M.C. Whiting, R.B. Woodward, J. Am. Chem. Soc. 74 (1952) 2125.
[3] P.L. Pauson, J. Organomet. Chem. 3 (2001) 637–639.
[4] M.E. Rerek, F. Basolo, J. Am. Chem. Soc. 106 (1984) 5908.
[5] H. Sitzmann, Coord. Chem. Rev. 214 (2001) 287.
[6] O.T. Summerscales, F.G.N. Cloke, Coord. Chem. Rev. 250 (2006) 1122.
[7] M.J. Calhorda, V. Felix, L.F. Veiros, Coord. Chem. Rev. 230 (2002) 49.
[8] D. Zargarian, Coord. Chem. Rev. 233 (2002) 157.
[9] M. Stradiotto, M.J. McGlinchey, Coord. Chem. Rev. 219 (2004) 311.
[10] A. Ceccon, S. Santi, L. Orian, A. Bisello, Coord. Chem. Rev. 248 (2004) 683.
[11] P.J. Chirik, Organometallics 29 (2010) 1500.
[12] S. Bendjaballah, S. Kahlal, K. Costuas, E. Be villon, J.-Y. Saillard, Chem. Eur. J. 12 (2006) 2048.
[13] H. Korichi, F. Zouchoune, S.-M. Zendaoui, B. Zouchoune, J.-Y. Saillard, Organometallics 29 (2010) 1693.
[14] M.J. Calhorda, L.F. Veiros, J. Organomet. Chem. 635 (2001) 197.
[15] L.F. Veiros, Chem. Eur. J. 11 (2005) 2505.
[16] L.F. Veiros, Organometallics 25 (2006) 2266.
[17] C.A. Bradley, L.F. Veiros, D. Pun, E. Lobkovsky, I. Keresztes, P.J. Chirik, J. Am. Chem. Soc. 128 (2006) 16600.
[18] C.A. Bradley, L.F. Veiros, P.J. Chirik, Organometallics 26 (2007) 319.
[19] F. Chekkal, S.M. Zendaoui, B. Zouchoune, Jean-Yves Saillard, New J. Chem. 37 (2013) 2293–2302.
[20] S. Farah, S. Ababsa, N. Benhamada, B. Zouchoune, Polyhedron 29 (2010) 2722–2730.
[21] Naïma Bouchakri, A. Benmachiche, B. Zouchoune, Polyhedron 30 (2011) 2644–2653.
[22] A. Benmachiche, S.M. Zendaoui, S.E. Bouaoud, B. Zouchoune, Int. J. Quant. Chem. 113 (2013) 985–996.
[23] S. Farah, N. Bouchakri, S.M. Zendaoui, J.Y. Saillard, B. Zouchoune, J. Mol. Struct. 953 (2010) 143–150.
[24] S. Farah, H. Korichi, S.M. Zendaoui, J.Y. Saillard, B. Zouchoune, Inorg. Chim. Acta 362 (2009) 3541–3546.
[25] T.J. Kaltz, J. Schulman, J. Am. Chem. Soc. 86 (1964) 3169.
[26] T.J. Kaltz, N. Acton, J. Am. Chem. Soc. 94 (1972) 3281. T.J. Kaltz, N. Acton, J. McGinnis, J. Am. Chem. Soc. 94 (1972) 6205.
[27] D.J. Brauer, C. Kruger, J. Organomet. Chem. 122 (1976) 265.
[28] M. Horacek, V. Kupfer, U. Thewalt, P. Stepnicka, M. Polasek, K. Mach, J. Organomet. Chem. 584 (1999) 286.
[29] G. Balazs, F.G.N. Clock, L. Gagliardi, J.C. Green, A. Harrison, P.B. Hitchcock.
[30] A.R.M. Shahi, O.T. Summerscales, Organometallics 27 (2008) 2013–2020.
[31] G. Balazs, F.G.N. Clock, A. Harrison, P.B. Hitchcock, J.C. Green, O.T. Summerscales, Chem. Commun. (2007) 873.
[32] M.C. Kuchta, F.G.N. Clock, P.B. Hitchcock, Organometallics 17 (1998) 1934.
[33] F.G.N. Clock, J.C. Green, C.N. Jardine, M.C. Kuchta, Organometallics 18 (1999) 1087.
[34] A.E. Ashley, R.T. Cooper, G.G. Wildgoose, J.C. Green, D. O'Hare, J. Am. Chem. Soc. 13 (2008) 15662.
[35] K. Jonas, W. Rüsseler, C. Krüger, E. Raabe, Angew. Chem. Int. Ed. Engl. 25 (1986) 928.
[36] J.C. Smart, B.L. Pinsky, J. Am. Chem. Soc. 99 (1977) 956.
[37] J.C. Smart, B.L. Pinsky, M.F. Fredrih, V.W. Day, J. Am. Chem. Soc. 101 (1979) 4371.
[38] H.L. Fernando, C.A. Bradely, Organometallic 30 (2011) 2636–2639.
[39] T. Murahashi, S. Kimura, K. Takase, T. Uemura, S. Ogoshi, K. Yamamoto, Chem. Commun. 50 (2014) 820–822.
[40] T. Murahashi, T. Uemura, H. Kurosawa, J. Am. Chem. Soc. 125 (2003) 8436–8437.
[41] T. Murahashi, R. Inoue, K. Usui, S. Ogoshi, J. Am. Chem. Soc. 131 (2009) 9888–9889.
[42] T. Murahashi, N. Kato, T. Uemura, H. Kurosawa, Angew. Chem. Int. Ed. Engl. 46 (2007) 3509–3512.
[43] G. Zhu, J.M. Tanski, D.G. Churchil, K.E. Janak, G. Parkin, J. Am. Chem. Soc. 124 (2002) 13658–13659.
[44] R.A. Sanchez-delgado, Organometallic Modeling of the Hydride Sulfonisation and Hydrodenitrogenation Reactions, Kluwer Academic Publishers, Boston, 2002.
[45] I.N. Ji, D.I. Kershner, M.E. Rerek, F. Basolo, J. Organomet. Chem. 296 (1985) 83.
[46] L. Gagliardi, P. Pyykkö, J. Am. Chem. Soc. 123 (2001), 9700–9701.
[47] A.C. Tsipis, A. Th. Chavaria, Inorg. Chem. 43 (2004) 1273–1286.
[48] A. Sattler, G. Zhu, G. Parkin, J. Am. Chem. Soc. 131 (2009) 7828.
[49] S.M. Zendaoui, B. Zouchoune, Polyhedron 51 (2013) 123–131.
[50] F. Weinhold, C.R. Landis, Valency and Bonding: a Natural Bond Order Donor–Acceptor Perspective, Cambridge University Press, U. K., 2005.
[51] E.D. Glendening, J.K. Badenhoop, A.E. Reed, J.E. Carpenter, J.A. Bohmann, C.M. Morales, F. Weinhold, Natural Bond Orbitals "Analysis Programs" Theoretical Chemistry Institute, University of Wisconsin, Madison, WI, 2001.
[52] V. Shuster, S. Gambarotta, G.B. Nikiforov, P. Budzelaar, Organometallics 32 (2013) 2329–2335.
[53] D. Seyferth, Organometallics 21 (2002) 1520–1530.
[54] D. Seyferth, Organometallics 21 (2002) 2800–2820.
[55] T. Ziegler, A. Rauk, Theor. Chem. Acta 46 (1977) 1.
[56] T. Ziegler, A. Rauk, Inorg. Chem. 18 (1979) 1558.
[57] K.B. Lipkowitz, D.B. Boyd (Eds.), vol. 15, Wiley-VCH, New York, 2000, pp. 1–86.
[58] A.W. Ehlers, S. Dapprich, S.F. Vyboishchikov, G. Frenking, Organometallics 15 (1996) 105.
[59] ADF2007.01, Theoretical Chemistry, Vrije Universiteit: Amsterdam, The Netherlands, SCM.
[60] E.J. Baerends, D.E. Ellis, P. Ros, Chem. Phys. 2 (1973) 41–51.
[61] G. te Velde, E.J. Baerends, J. Comput. Phys. 99 (1992) 84–98.
[62] C. Fonseca Guerra, J.G. Snijders, G. te Velde, E.J. Baerends, Theor. Chim. Acc. 99 (1998) 391–403.
[63] F.M. Bickelhaupt, E.J. Baerends, Rev. Comput. Chem. 15 (2000) 1–86.
[64] G. te Velde, F.M. Bickelhaupt, C. Fonseca Guerra, S.J.A. van Gisbergen, E.J. Baerends, J.G. Snijders, T. Ziegler, J. Comput. Chem. 22 (2001) 931–967.
[65] S.D. Vosko, L. Wilk, M. Nusair, Can. J. Chem. 58 (1990) 1200–1211.
[66] A.D. Becke, J. Chem. Phys. 84 (1986) 4524–4529.
[67] A.D. Becke, Phys. Rev. A 38 (1988) 3098–3100.
[68] J.P. Perdew, Phys. Rev. B 33 (1986) 8822–8824.
[69] J.P. Perdew, Phys. Rev. B 34 (1986) 7406.
[70] L. Versluis, T. Ziegler, J. Chem. Phys. 88 (1988) 322–329.
[71] L. Fan, T. Ziegler, J. Chem. Phys. 96 (1992) 9005–9012.
[72] L. Fan, T. Ziegler, J. Phys. Chem. 96 (1992) 6937–6941.
[73] P. Flükiger, H.P. Lüthi, S. Portmann, J. Weber, MOLEKEL, Version 4.3.win32, Swiss Center for Scientific Computing (CSCS), Switzerland, 2000–2001. http://www.cscs.ch/molekel/. http://www.cscs.ch/molekel/.